Electronic Supplementary Material (ESI) for Journal of Materials Chemistry A.

Supplementary Information

Highly Efficient Removal of Cs^+ from Water by Ionic Lamellar Carbon Nitride Framework

Zhenchun Yang,[a] Bixiao Guo,[b] Zhenyu Hu,[a] Jiahao Cui,[a] Jianguo Cui,[c] Lina Li,[a] Chun Hu,[a] Yubao Zhao[a,] *

[a] Key Laboratory for Water Quality and Conservation of the Pearl River Delta, Ministry of Education, Institute of Environmental Research at Greater Bay, Guangzhou University, 510006 Guangzhou, P. R. China

[b] Department of Environmental Science and Engineering, Guangzhou University, 510006 Guangzhou, P. R. China

[c] Baotou Research Institute of Rare Earths, 014030 Baotou, P. R. China.

* **Email: ybzhao@gzhu.edu.cn** (Y. Zhao)

Table of Content

Cs^+ removal via ion exchange

In the kinetic studies, 20 mg of CN-Na was dispersed in 40 mL of CsCl solution with concentration of 0.5 mM and magnetically stirred at room temperature. The solution was sampled at specified time intervals (0, 5, 10, 15, 20, 30, 45, 60, 90, 120 min). The solid sample was separated from the liquid phase by PTEF syringe filter. The concentrations of Cs^+ in the liquid phase were analyzed by inductively coupled plasma-optical emission spectroscopy (ICP-OES).

Absorption isotherm measurement. 20 mg of CN-Na was mixed with 40 mL aqueous solution with a series of Cs^+ concentrations (0.01 mM ~ 5 mM) and magnetically stirred for 2 h at room temperature to reach the absorption equilibrium. The concentration of Cs^+ remaining in the liquid phase was analyzed by ICP-OES.

Cs^+ removal by CN-Na in ion-exchange column. 1g CN-Na was loaded in a glass column. The solution with Cs^+ concentration of 0.5 mM was pumped into the ion-exchange column at the flow rate of 0.5 mL min^{-1} by a peristaltic pump. The concentration of Cs^+ in the effluent was determined by ICP-OES.

Regeneration of the ion-exchange column. An aqueous NaCl solution with concentration of 10 wt.% was pumped into ion-exchange column to regenerate the column. The column was flushed with water before being applied in the next cycle ion exchange process to remove Cs^+.

The remove rate $\mathbf{R^{Cs}}$ (%) is used to evaluate the removal efficiency of Cs^+:

$$R^{Cs} = \frac{C_o - C_e}{C_o} \times 100\% \quad \text{eq. 1}$$

wherein C_o is the 0.5 mM (initial Cs^+ concentration), C_e is the Cs^+ concentration under absorption equilibrium in the ion exchange experiment.

Kinetic curves models

Pseudo-first-order kinetics model:

$$\lg (q_e - q_t) = \lg q_e - \frac{k_1}{2.303} t$$

Pseudo-second-order kinetics model:

$$\frac{t}{q_t} = \frac{1}{k_2 q_e^2} + \frac{t}{q_e}$$

q_e (with unit of mg g^{-1}) is the ion exchange capacities under absorption equilibrium. q_t is ion exchange capacities at time t (with unit of min). k_1 (with unit of min^{-1}) and k_2 (with unit of g mg^{-1} min^{-1}) are, respectively, the rate constants in the pseudo-first-order and pseudo-second-order kinetics models.

Absorption isotherm models

Langmuir isotherm model:

$$q = q_m \frac{bC_e}{1 + bC_e}$$

q_m (with unit of mg g^{-1}) is the maximum ion exchange capacity, b (with unit of L mg^{-1}) is the Langmuir constant, C_e (with unit of mg L^{-1}) is the equilibrium concentration of Cs^+ at ion exchange experiment.

Freundlich isotherm model:

$$q = K_F C_e^{1/n}$$

K_F and $1/n$ are the Freundlich constants, C_e (with unit of mg L^{-1}) is the equilibrium concentrations in the ion exchange experiment.

Langmuir-Freundlich isotherm model:

$$q = q_m \frac{(bC_e)^{1/n}}{1 + (bC_e)^{1/n}}$$

q_m (with unit of mg g^{-1}) is the maximum ion exchange capacity, b (with unit of L mg^{-1}) is the Langmuir constant, C_e (with unit of mg L^{-1}) is the equilibrium concentrations of Cs^+ in the ion exchange experiment. *1/n* is the Freundlich constant.

Characterizations

The morphology of the materials was characterized by transmission electron microscopy (JEOL 2100F). X-ray diffraction patterns of the materials were obtained on a PANalytical PW3040/60 diffractometer with Cu radiation (Cu Kα = 0.15406 nm). X-ray photoelectron spectroscopy (XPS) patterns were recorded on an ESCA laboratory 220i-XL spectrometer with an Al Kα (1486.6 eV) X-ray source and a charge neutralizer; all the binding energy were calibrated to C 1s peak at 284.8 eV. Infrared spectrometry of the materials was measured on the Thermo scientific Nicolet IS50 ATR FT-IR. The surface charge state of sample was measured on Zeta potential analyzer ELSZ-2000Z.

Theoretical simulations

The theoretical simulation was performed by using the Vienna ab initio Simulation Program (VASP). The generalized gradient approximation (GGA) in the Perdew-Burke-Ernzerhof (PBE) form and a cutoff energy of 500 eV for planewave basis set were used. A 5 × 5 × 1 Monkhorst-Pack k grid was employed for sampling the Brillouin zones at structure calculation. The ion-electron interactions were analyzed via the method of the projector augmented wave (PAW). The convergence criteria of structure optimization were selected as the maximum force on each atom less than 0.02 eV/Å with an energy change less than 1×10^{-5} eV.

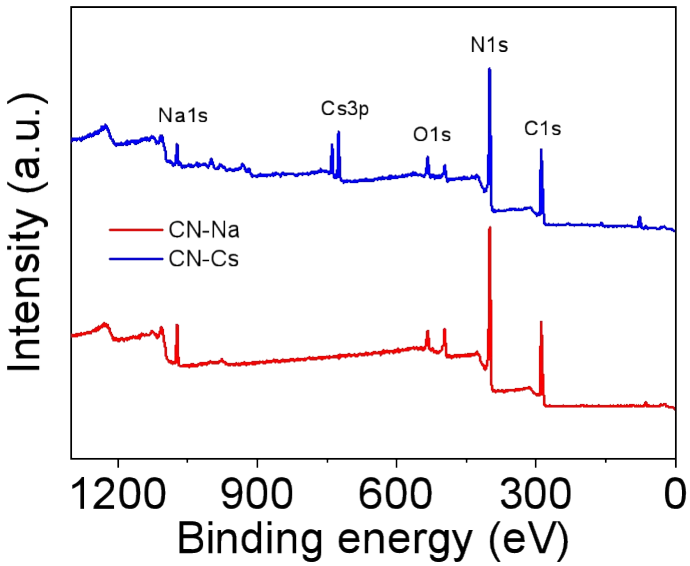

Figure S1. XPS survey scans on CN-Na and CN-Cs.

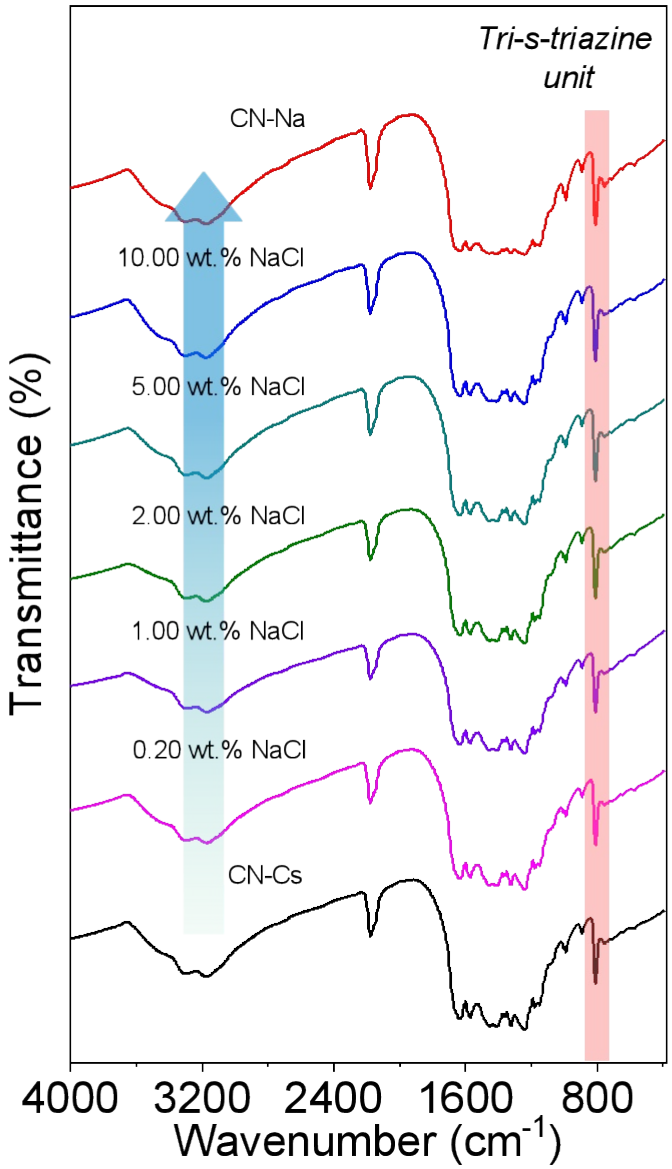

Figure S2. FT-IR spectra investigations on CN-Cs to CN-Na recovery.

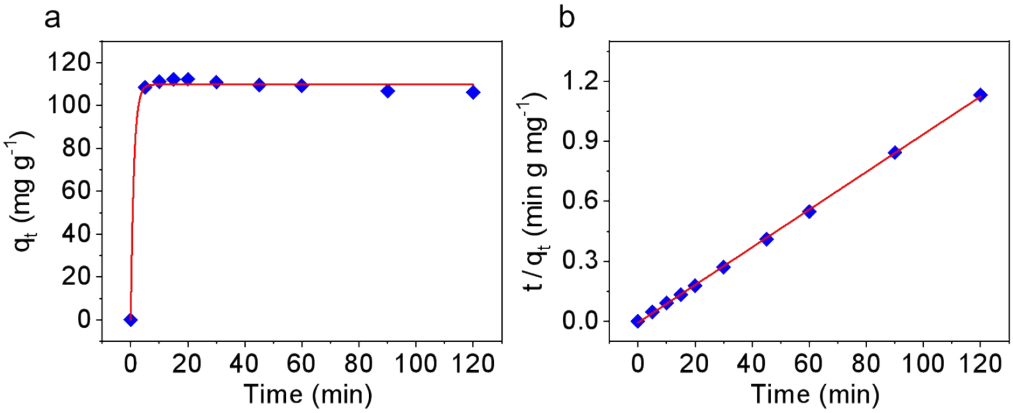

Figure S3. Kinetic fitting of the Cs^+ absorption process. (a) Pseudo-first-order and (b) pseudo-second-order kinetics models fitted curves for the data of Cs ion exchange by CN-Na.

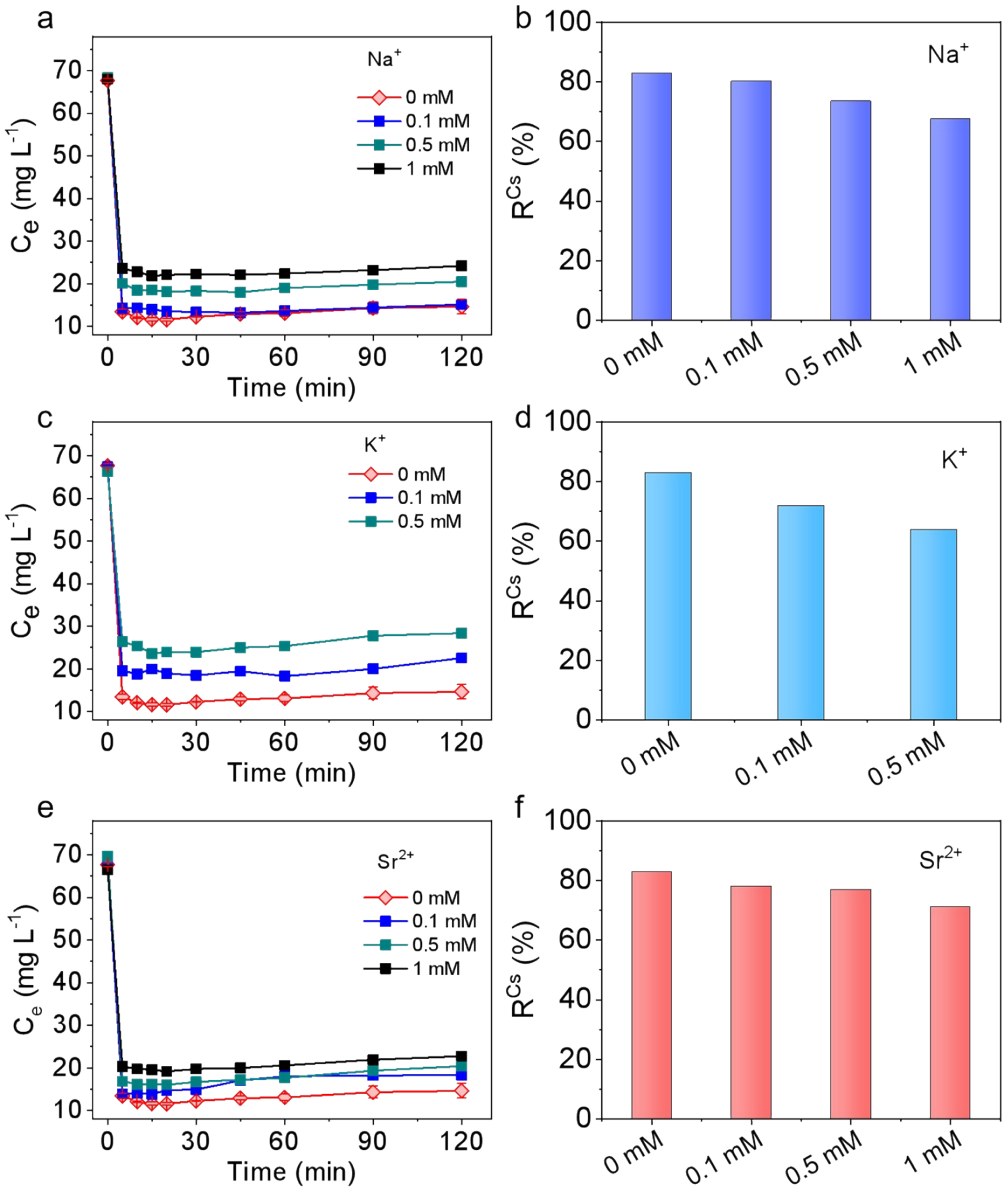

Figure S4. Cs^{+} removal performance of CN-Na in the presence of Na^{+}, K^{+}, and Sr^{2+}.

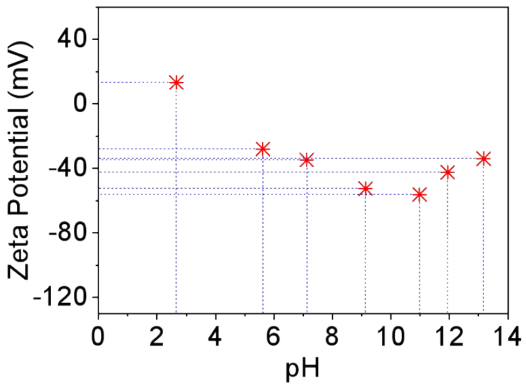

Figure S5. Zeta potential of CN-Na in the solution at a series of pH.

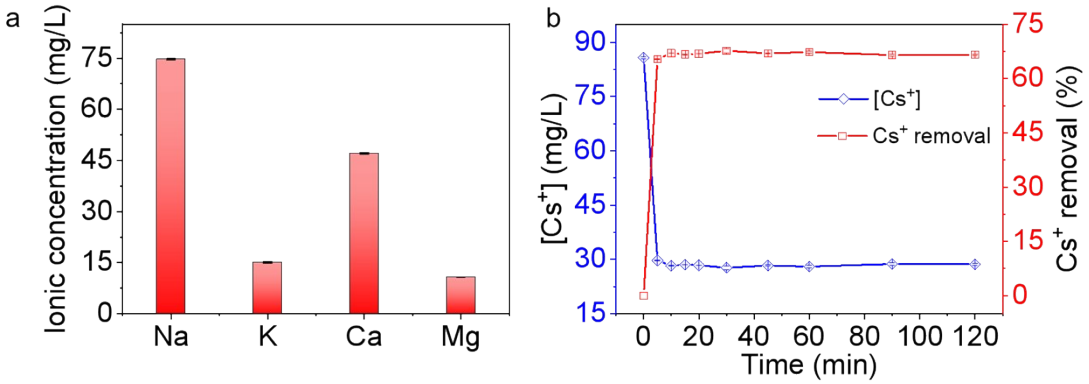

Figure S6. (a) The ionic concentration of Na, K, Ca and Mg in actual water from the Pearl River (Guangzhou, P. R. China). (b) Kinetic plots of the Cs^+ uptake by CN-Na in actual water. Initial $[Cs^+]$ = 85.8 mg L^{-1}.

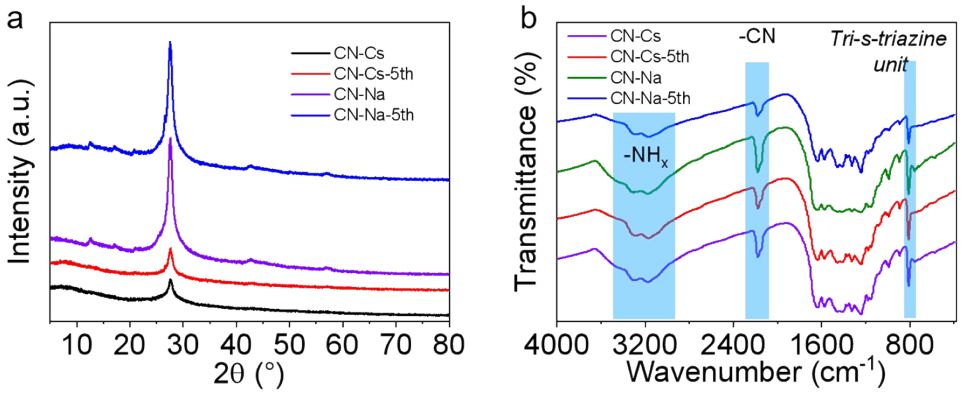

Figure S7. Comparison of the recycled materials with the pristine ones. (a) X-ray diffraction (XRD) patterns, (b) Fourier-transform Infra-red (FT-IR) spectra.

Table S1. Comparison of Cs^+ remove efficiency of CN-Na with the other adsorbents.

Sample	Absorbent loading ($g\ L^{-1}$)	[Cs^+] ($mg\ L^{-1}$)	Equilibrium time (min)	Removal efficiency (%)	Ref.
CN-Na	0.5	65	5	80.1	This work
$[(CH_3)_2NH_2]_4[(UO_2)_4(TBAPy)_3]\cdot 22DMF\cdot 37H_2O$	1	1	20	89.0	1
AAC	0.7	100	1440	58.0	2
SAC	0.7	100	1440	63.0	
AgSnSe-1	1	6	60	70.1	3
FJSM-InMOF	0.4	90	60	83.0	4
			180	91.7	
DGIST-2'⊃methanol	0.66	115	15	57.9	5
FJSM-SnS-4	1	11.2	2	60.71	6
			30	78.57	
FJSM-SnS/PAN	1	9.32	10	55.26	7
			90	77.25	
FJSM-SnS-2	1	0.73	60	83.0	8
FJSM-SnS-3	1	0.778	60	75.0	
FJSM−SbS	1	0.6168	2	86.93	9
$[(CH_3)_2NH_2]In(aip)_2\cdot DMF\cdot H_2O$	1	6.5	1	92.92	10
$[(CH_3)_2NH_2]In(hip)_2\cdot DMF\cdot H_2O$	1	3.9	1	89.23	
InSnS-1 (Nature)	1	3.44	5	91.28	11
InSnS-1 (1 M HNO_3)	1	4.3	20	82.33	
KIAS	1	2.05	1	92.98	12
SbS-1K	1	6	2	93.29	13
			5	97.40	

Table S2. Kinetic fitting parameters of the Cs^+ absorption process by CN-Na .

	Pseudo-first-order model			Pseudo-second-order model		
CN-Na	**k_1 (min^{-1})**	**q_m (mg g^{-1})**	**R^2**	**k_2 (g mg^{-1} min^{-1})**	**q_m (mg g^{-1})**	**R^2**
	0.8877	109.80	0.9961	0.01273	106.16	0.9997

Table S3. Parameters of the fitting based on Langmuir, Freundlich and Langmuir-Freundlich models.

Model	Parameter	Value
Langmuir	q_m (mg g^{-1})	241.25
	b (L mg^{-1})	0.0516
	R^2	0.974
Freundlich	K_F	55.88
	n	4.08
	R^2	0.932
Langmuir-Freundlich	q_m (mg g^{-1})	278.20
	b (L mg^{-1})	0.0362
	n	1.565
	R^2	0.993

Table S4. Compared the Cs ion exchange capacity of CN-Na with other adsorbents.

Sample	pH	Temperature	q_m (mg g^{-1})	Ref.
CN-Na	9.8	Room temperature	278.2	This work
AAC	6.0	Room temperature	362	2
SAC	6.0	Room temperature	259	
AgSnSe-1	\	Room temperature	174.4	3
FJSM-InMOF	\	Room temperature	198.63	4
DGIST-2'⊃methanol	\	\	183	
DGIST-3-S	\	\	156	5
DGIST-2'⊃water	\	\	164	
FJSM-SnS-4	7.1	298 K	388.94	6
	0.4	298 K	137.07	
	1.6	298 K	167.72	
FJSM-SnS/PAN	7.1	Room temperature	296.12	7
	2.5	Room temperature	89.29	
FJSM-SnS-2	3.2-9.3	\	266.54	8
FJSM-SnS-3	3.2-9.3	\	109.68	
FJSM-SbS	\	353 K	146.12	9
$[(CH_3)_2NH_2]In(aip)_2 \cdot DMF \cdot H_2O$	\	Room temperature	297.67	10
$[(CH_3)_2NH_2]In(hip)_2 \cdot DMF \cdot H_2O$	\	Room temperature	295.82	
InSnS-1	Neutral	Room temperature	316.04	11
	1 M HNO_3	Room temperature	98.57	
SbS-1K	0-12	293 K	318.77	13
DIMS-2	6.0	298.15	34.5	14
FJSM-GAS-1	4-7	\	164	15
NaMT-S20	8.0	298 K	160.9	16
GAPP	6.0	298.15 K	163.6	17

References

1 J. Ai, F. Y. Chen, C. Y. Gao, H. R. Tian, Q. J. Pan and Z. M. Sun, *Inorg. Chem.*, 2018, **57**, 4419-4426.

2 A. Baimenov, F. Montagnaro, V. J. Inglezakis and M. Balsamo, *Ind. Eng. Chem. Res.*, 2022, **61**, 8204-8219.

3 D. Ding, L. Cheng, K. Y. Wang, H. W. Liu, M. Sun and C. Wang, *Inorg. Chem.*, 2020, **59**, 9638-9647.

4 Y.-J. Gao, M.-L. Feng, B. Zhang, Z.-F. Wu, Y. Song and X.-Y. Huang, *J. Mater. Chem. A*, 2018, **6**, 3967-3976.

5 K. Jin, X. Q. Wu, Y. P. Chen, I. H. Park, J. R. Li and J. Park, *Inorg. Chem.*, 2022, **61**, 1918-1927.

6 J. Li, J. Jin, T. Zhang, W. Ma, X. Zeng, H. Sun, M. Cheng, M. Feng and X. Huang, *ACS EST Water*, 2021, **1**, 2440-2449.

7 J. Li, J. Jin, Y. Zou, H. Sun, X. Zeng, X. Huang, M. Feng and M. G. Kanatzidis, *ACS Appl. Mater. Interfaces*, 2021, **13**, 13434-13442.

8 W. A. Li, J. R. Li, B. Zhang, H. Y. Sun, J. C. Jin, X. Y. Huang and M. L. Feng, *ACS Appl. Mater. Interfaces*, 2021, **13**, 10191-10201.

9 Y. Y. Liao, J. R. Li, B. Zhang, H. Y. Sun, W. Ma, J. C. Jin, M. L. Feng and X. Y. Huang, *ACS Appl. Mater. Interfaces*, 2021, **13**, 5275-5283.

10 W. Ma, T. T. Lv, J. H. Tang, M. L. Feng and X. Y. Huang, *JACS Au*, 2022, **2**, 492-501.

11 J. H. Tang, J. C. Jin, W. A. Li, X. Zeng, W. Ma, J. L. Li, T. T. Lv, Y. C. Peng, M. L. Feng and X. Y. Huang, *Nat. Commun.*, 2022, **13**, 658.

12 X. Zeng, M. Zeng, P.-W. Cai, J.-H. Tang, W. Ma, M.-L. Feng and X.-Y. Huang, *Environ. Sci. Adv.*, 2022, **1**, 331-341.

13 Y. M. Zhao, L. Cheng, K. Y. Wang, X. Hao, J. Wang, J. Y. Zhu, M. Sun and C. Wang, *Adv Funct Mater*, 2022, **32**, 2112717.

14 L. Zhou, M. Xu, J. Yin, R. Shui, S. Yang and D. Hua, *ACS Appl. Mater. Interfaces*, 2021, **13**, 6322-6330.

15 M. L. Feng, D. Sarma, Y. J. Gao, X. H. Qi, W. A. Li, X. Y. Huang and M. G. Kanatzidis,

J. Am. Chem. Soc., 2018, **140**, 11133-11140.

16 S. Chen, J. Hu, G. Mi, Y. Guo and T. Deng, *Green Energy Environ.*, 2021, **6**, 893-902.

17 S. Chen, J. Hu, Y. Guo and T. Deng, *Sci. Rep.*, 2020, **10**, 8221.